Progress Toward Corrugated Feed Horn Arrays in Silicon

J. Britton, K. W. Yoon, J. A. Beall, D. Becker, H. M. Cho, G. C. Hilton, M. D. Niemack and K. D. Irwin

Quantum Sensors Group, NIST, Boulder, CO 80305, USA

Abstract. We are developing monolithic arrays of corrugated feed horns fabricated in silicon for dual-polarization single-mode operation at 90, 145 and 220 GHz. The arrays consist of hundreds of platelet feed horns assembled from gold-coated stacks of micro-machined silicon wafers. As a first step, Au-coated Si waveguides with a circular, corrugated cross section were fabricated; their attenuation was measured to be less than 0.15 dB/cm from 80 to 110 GHz at room temperature. To ease the manufacture of horn arrays, electrolytic deposition of Au on degenerate Si without a metal seed layer was demonstrated. An apparatus for measuring the radiation pattern, optical efficiency, and spectral band-pass of prototype horns is described. Feed horn arrays made of silicon may find use in measurements of the polarization anisotropy of the cosmic microwave background radiation.

Keywords: millimeter wave optics, observational cosmology, MEMs
PACS: 95.85.Bh, 98.80.Es, 07.57.Kp

Imaging detectors at millimeter wavelengths can now be built with hundreds of pixels [1]. However, parallel gains in free-space coupling optics have lagged.

At NIST we are pursuing monolithic arrays of corrugated platelet feed horns made with Si. Each layer in the stack is a Si wafer with photolithographically defined apertures. Once assembled and coated with Au, these horn arrays are expected to feature the same low loss, wide bandwidth, minimal side lobes and low cross-correlation as electroformed horns [2, 3]. Moreover, relative to metal corrugated arrays [4], Si horn arrays are expected to have the following benefits: (a) a thermal expansion matched to Si detectors, (b) lower thermal mass, and (c) straightforward development to arrays of thousands of horns. The foremost of these considerations means that detector-horn alignment at room temperature should be maintained at low temperature (Table 1). Silicon is also convenient due to the availability of high resolution wafer-scale Si etch tools.

To demonstrate the feasibility of this approach we fabricated W-band (WR10) waveguides out of Si and measured their transmission characteristics from 80 to 110 GHz. The Si platelets were machined in 76.2 mm diameter Si wafers by use of photolithography and deep reactive ion etching (DRIE). In 250 μm thick Si, for example, features can be reproduced with $\sim 5\,\mu$m lateral resolution through the full wafer bulk ($\sim 50:1$ aspect ratio). Sidewall roughness for etched apertures is less than 1 μm [5]. Tools for applying this process to wafers 150 mm in diameter are currently being installed at NIST.

With the aim of easing the eventual manufacture of horn arrays, we demonstrated electrolytic deposition of Au films directly on degenerate Si. Tests of film adhesion and waveguide performance are reported.

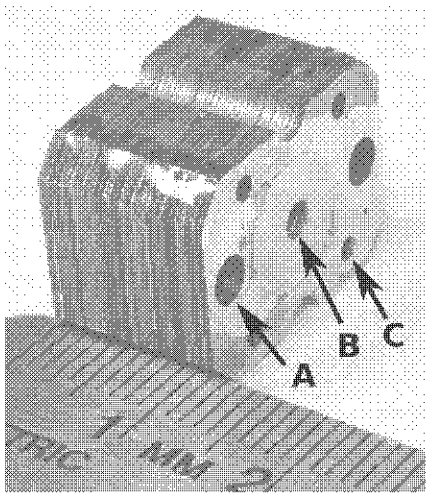

FIGURE 1. Photograph of an assembled circular waveguide after electroplating with Au. Visible in the figure are features for joining the Si waveguide with other standard metallic waveguide components: A) clearance holes for 4 – 40 screws and C) four holes for stainless alignment dowels. Arrow B identifies the waveguide channel. The shiny surface is dried epoxy used to hold the stack together. The annulus surrounding the waveguide (B) is an artifact of the electroplating process and is not functional.

An apparatus was constructed to measure the far-field radiation pattern and cross polarization of feed horns by use of a vector network analyzer.

CP1185, *Low Temperature Detectors LTD 13, Proceedings of the 13th International Workshop*
edited by B. Cabrera, A. Miller, and B. Young
2009 American Institute of Physics 978-0-7354-0751-0/09/$25.00

TABLE 1. Comparison of materials for horn arrays. Where, c_p is specific heat and α is coefficient of thermal expansion [6].

	$c_p/(\mathrm{J}\cdot\mathrm{g}^{-1}\cdot\mathrm{K}^{-1})$ at 77 K	$\alpha/(1\times10^{-6}/K^{-1})$ at 293 K
Al	0.336	23.1
Mg	0.488	8.2
Be	0.080	11.3
Cu	0.195	16.5
Si	0.18	2.6

CIRCULAR WAVEGUIDES

A pair of waveguides with circular cross section were assembled from platelets 380 μm thick. The waveguide apertures were sized to be single mode from 80 to 110 GHz. One waveguide was smooth-walled (2.21 mm diameter; 4.0 mm length) and one was corrugated (2.1/5.55 mm diameter, alternating every 380 μm; 11.5 mm length). The corrugation depth was one half-wavelength deep. A metal seed layer (Ti:Au 100 nm:500 nm) was deposited on platelets mounted on an orbital platform canted at 45°. Platelets were stacked on alignment pins and adhered with two-part epoxy applied to their edges. Platelet alignment accuracy was $\pm10\,\mu$m. Subsequent electrolytic plating of the assembled stack increased the Au thickness to $3-5\,\mu$m on flat surfaces (less in the corrugations). Figure 1 shows a photograph of one waveguide structure.

Waveguide loss was measured by use of a vector network analyzer (VNA). A short followed the device under test so that a S11 reflection measurement gave twice the single-pass loss. We observed less than 0.15 dB/cm loss in both the corrugated and not corrugated waveguides (Fig. 3). We also measured the transmission (S12) for the waveguides and observed attenuation consistent with the S11 measurements.

It is instructive to compare the loss in our circular corrugated waveguides with the expected loss α for the fundamental (TE_{10}) mode of a hollow rectangular waveguide due to finite wall conductivity. An expression for α is

$$\alpha=\frac{\lambda_0}{b\lambda_g}\sqrt{\frac{\pi}{\lambda_0\eta\sigma}}\left(1+\left(\frac{\lambda_g}{\lambda_c}\right)^2\left(1+2\frac{b}{a}\right)\right)\times8.676\,\mathrm{dB/m}, \quad (1)$$

where $\lambda_0=c/f$ is the free-space wavelength, c is the speed of light, f is the frequency, $\lambda_g=\lambda_0/\sqrt{1-(\lambda_0/\lambda_c)^2}$ is the guided wavelength, $\lambda_c=2a$ is the waveguide cutoff wavelength, $\eta=\sqrt{\mu_0/\varepsilon_0}$ is the intrinsic impedance of the material filling the waveguide (vacuum), σ is the conductivity, and a and b are the width and height of the waveguide cross section [7]. For $f=100\,\mathrm{GHz}$, $\sigma_{Au}=2.05\times10^{-8}\,\Omega\cdot\mathrm{m}$ (at 273 K), $a_{WR10}=2.54$ mm and $b_{WR10}=1.27$ mm, $\lambda_0=3\,\mathrm{mm}$, $\lambda_g=3.7\,\mathrm{mm}$, $\lambda_c=5.1\,\mathrm{mm}$ ($f_c=59\,\mathrm{GHz}$) and $\eta=377\,\Omega$ we have $\alpha=0.027$ dB/cm. Note that the surface resistance of Au drops by over a factor of 10 from room temperature to 10 K [8]. The excess conduction loss we observe may be caused by metal surface roughness and scattering into non-propagating modes [9]. In our guides the latter is expected to dominate and therefore we do not expect a large reduction in loss if the waveguides were tested at 10 K.

To test whether the waveguide attenuation plotted in Fig. 3 was limited by plating thickness, an additional layer of Cu 3 to 5 μm thick followed by Au 1 to 2 μm thick was deposited (as measured on flat, superficial surfaces; e.g., location B in Fig. 2). Following this treatment there was no change in attenuation. This is to be expected because the skin depth of bulk Au at 100 GHz and 273 K (78 K) is 90 nm (43 nm) [6, 10].

ELECTROLYTIC PLATING OF DEGENERATE SI

Low transmission losses in our Si waveguides were obtained by electroplating with Au, a chemistry that requires that the target surface be initially conducting. In the devices described in the previous section, we achieved this by e-beam evaporation of a Ti:Au (100 nm:500 nm) seed layer prior to electroplating. This step could be eliminated by use of degenerate Si as a substrate material. Degenerate Si with a bulk resistivity of less than $50\times10^{-6}\,\Omega\cdot\mathrm{m}$ is available commercially. For such a wafer with a substrate thickness of 100 μm, the sheet resistance is $100\times10^{-3}\,\Omega/\square$, equivalent to a 200 nm Au seed layer [6]. On test chips made of Si we successfully demonstrated Au deposition based on a recipe by Llona, *et al* [11].

The electrolytic deposition rate depends on geometry via the local electric field and depletion of the plating solution. Corrugated waveguides have recesses that might plate more slowly than exposed surfaces. To test this we microfabricated, then electroplated, Si test structures (Fig. 2) with linear trenches whose aspect ratios (depth/width) varied from 0.44 to 8.75. After snapping a sample wafer perpendicular to a row of such trenches, the deposition thickness was measured from SEM micrographs near the bottom of the trenches. Over this range of aspect ratios, the plating rate diminished from 1/2 to 1/5 (C to D in Fig. 2) of the rate at the top surface (B in Fig. 2).

The adhesion of Au electrolytically deposited on degenerate Si was investigated. Three tests were conducted: chips were (a) scratched with stainless forceps, (b) dipped repeatedly in liquid nitrogen, and (c) snapped

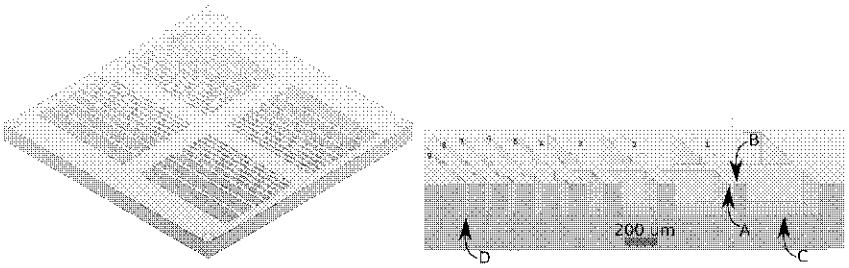

FIGURE 2. (top) Schematic view of a test chip for electrolytic plating of Au directly on degenerate Si ($0.5\,\mathrm{cm}^2$). The Si was $400\,\mu$m thick, B-doped (p-type), $\sigma \quad 10 \times 10^{-6}\,\Omega \cdot$ m. (bottom) Trenches were deep etched into the Si surface to mimic the aspect ratio (depth/width) of corrugations in a waveguide. The trench depth is about $175\,\mu$m deep. From right to left, the widest trench is $400\,\mu$m wide, the narrowest is $20\,\mu$m wide. (B) denotes the top surface of the chip with zero aspect ratio, while (D) marks a trench with an aspect ratio of 8.75. Disregard (A). A waveguide with corrugations $\lambda/4$ deep repeated N times per λ has an aspect ratio of $N/2$. In our waveguides we aim for $N = 4$.

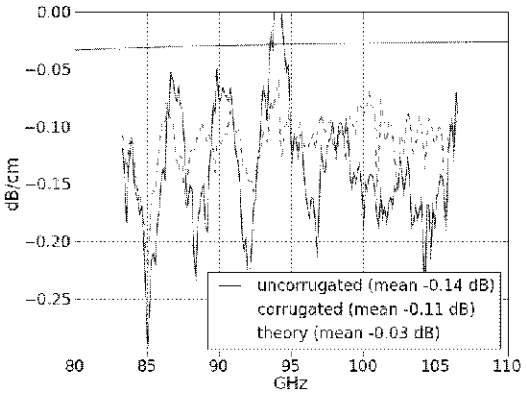

FIGURE 3. Attenuation for waveguides with circular cross section as determined by S11 measurements on a VNA. The baseline (0dB) was established by measuring S11 without a test waveguide installed. The vertical axis scaling relies on a calibration performed by the VNA manufacturer in 2008. The theory curve shows attenuation at room temperature due to finite conductivity of the waveguide walls assuming the bulk resistivity of Au ($\sigma_{Au} = 20.5 \times 10^{\ 9}\,\Omega \cdot$ m; see Eq. 1).

FIGURE 4. Micrograph of a degenerate Si electroplated with Au in cross section.

in half. No delamination of the Au was observed for the successful deposition recipe (Fig. 4).

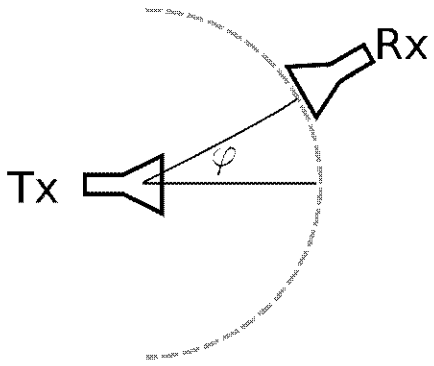

FIGURE 5. Schematic of feed horn test setup. It consists of two horns: a fixed transmitter (Tx) and a receiver (Rx) that pivots about the transmitter's phase center.

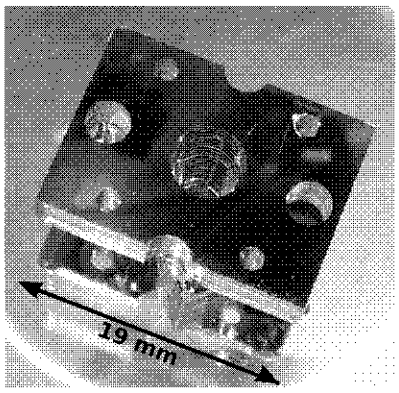

FIGURE 6. Photograph of a corrugated Si feed horn prior to metallization. This horn was designed for 145 GHz. Corrugations are visible in the central aperture as they extend downward into the stack. See Fig. 1 for an explanation of the visible hole pattern.

HORN TESTING APPARATUS

Desired characteristics of feed horns include low losses, wide bandwidth, minimal side lobes and low cross correlation of orthogonal polarizations. We built an apparatus to measure these parameters for horns we fabricated (Fig. 5). It consists of two horns: a fixed transmitter (Tx) and a receiver (Rx) that pivots about the transmitter's phase center. The Rx horn is a commercially manufactured corrugated metal horn for G-band (WR5). According to simulation, its cross polarization is less than 30 dB and side lobe amplitude is less than 25 dB at 150, 180 and 220 GHz. A vector network analyzer is used to measure S12 (amplitude and phase) as a function of angle (ϕ) and frequency. We use a 0° or 90° twist preceding the Tx horn to measure H-plane and E-plane mode patterns. Cross polarization measurements use 45° twists before the Tx horn and after the Rx horn. To confirm proper operation of the system we use a pair of identical metal horns. Return loss (insertion loss) is measured with the horn face pressed against a microwave absorber (metal plate). This apparatus is assembled and testing is underway.

CONCLUSION

In this proceeding we reported on progress toward fabrication of corrugated millimeter-wave feed horn arrays made of Si and a testing facility for evaluating the performance of millimeter-wave horns. Next steps include testing a 145 GHz Si feed horn (already designed and fabricated, Fig. 6) and demonstrating plating of a horn fabricated from degenerate Si. In 2009 we plan to build a prototype 75 mm diameter feed horn array, and in 2010 we plan to build a 150 mm diameter feed horn array with 640 channels (50 to 100 corrugations). Matching detectors and refractive optics will permit characterization of the imaging characteristics of these horn arrays.

ACKNOWLEDGMENTS

K. W. Yoon acknowledge support from the National Research Council. This work was supported by NIST through the Innovations in Measurement Science program. We thank Robbie Smith and Christian Wiggins who provided assistance developing the recipe for electrolytic plating of degenerate Si (Custom Microwave, Inc., Longmont, CO). This proceeding is a contribution of NIST and is not subject to U.S. copyright.

REFERENCES

1. K. W. Yoon, J. W. Appel, J. E. Austermann, J. A. Beall, D. Becker, B. A. Benson, L. E. Bleem, J. Britton, J. E. Carlstrom, C. L. Chang, H. M. Cho, A. T. Crites, W. Everett, T. Essinger-Hileman, N. W. Halverson, J. W. Henning, G. C. Hilton, K. D. Irwin, J. McMahon, J. Mehl, S. S. Meyer, M. D. Niemack, L. P. Parker, S. M. Simon, S. T. Staggs, C. Visnjic, K. Y. Yoon, and Y. Zhao, *LTD-13 proceedings* **this volume** (2009).
2. P. J. B. Clarricoats, and A. D. Olver, *Corrugated horns for microwave antennas*, Iet, 1984.
3. Y. T. Lo, and S. W. Lee, editors, *Antenna Handbook - Theory, Applications and Design*, Van Nostrand Reinhold Company, New York, 1988.
4. J. Bock, J. Gundersen, A. Lee, P. Richards, and E. Wollack, *Journal of Physics: Conference Series* **155**, 012005 (31pp) (2009), URL `http://stacks.iop.org/1742-6596/155/012005`.
5. S. A. McAuley, H. Ashraf, L. Atabo, A. Chambers, S. Hall, J. Hopkins, and G. Nicholls, *Journal of Physics D-Applied Physics* **34**, 2769–2774 (2001).
6. G. W. C. Kaye, and T. H. Laby, Tabes of physical and chemical constants (2009), URL `http://www.kayelaby.npl.co.uk/`.
7. A. J. B. Fuller, *Microwaves*, Permagon Press, 1979, 2nd edn.
8. R. C. Munoz, G. Vidal, M. Mulsow, J. G. Lisoni, C. Arenas, A. Concha, F. Mora, R. Espejo, G. Kremer, L. Moraga, R. Esparza, and P. Haberle, *Physical Review B* **62**, 4686 (2000).
9. E. J. Tischer, *IEEE T. Microw. Theory.* **24**, 853 (1976).
10. J. D. Jackson, *Classical electrodynamics*, Wiley, New York, 1999, 3rd ed edn., ISBN 047130932X (cloth : acid-free paper).
11. L. D. V. Llona, H. V. Jansen, and M. C. Elwenspoek, *Journal of Micromechanics and Microengineering* **16**, 1 (2006).